1-1-2013

Addressing retained austenite stability in advanced high strength steels

Elena V. Pereloma
University of Wollongong, elenap@uow.edu.au

Azdiar A. Gazder
University of Wollongong, azdiar@uow.edu.au

Ilana B. Timokhina
Deakin University, Ilana.Timokhina@eng.monash.edu.au

Addressing retained austenite stability in advanced high strength steels

Abstract

Advances in the development of new high strength steels have resulted in microstructures containing significant volume fractions of retained austenite. The transformation of retained austenite to martensite upon straining contributes towards improving the ductility. However, in order to gain from the above beneficial effect, the volume fraction, size, morphology and distribution of the retained austenite need to be controlled. In this regard, it is well known that carbon concentration in the retained austenite is responsible for its chemical stability, whereas its size and morphology determines its mechanical stability. Thus, to achieve the required mechanical properties, control of the processing parameters affecting the microstructure development is essential.

Keywords

strength, high, advanced, stability, austenite, steels, retained, addressing

Disciplines

Engineering | Science and Technology Studies

Publication Details

Pereloma, E. V., Gazder, A. A. & Timokhina, I. B. (2013). Addressing retained austenite stability in advanced high strength steels. Materials Science Forum, 738-739 212-216.

Addressing Retained Austenite Stability in Advanced High Strength Steels

Elena V. Pereloma[1,a], Azdiar A. Gazder[1,b] and Ilana B.Timokhina[2,c]

[1]School of Mechanical, Materials and Mechatronic Engineering, University of Wollongong, NSW 2522, Australia

[2]Centre for Material and Fibre Innovation, Deakin University, Geelong, VIC 3217, Australia

[a]elenap@uow.edu.au, [b]azdiar@uow.edu.au, [c]ilana.timokhina@monash.edu.au

Keywords: transformation-induced plasticity steel; retained austenite, chemical stability, mechanical stability, electron microscopy, mechanical properties.

Abstract. Advances in the development of new high strength steels have resulted in microstructures containing significant volume fractions of retained austenite. The transformation of retained austenite to martensite upon straining contributes towards improving the ductility. However, in order to gain from the above beneficial effect, the volume fraction, size, morphology and distribution of the retained austenite need to be controlled. In this regard, it is well known that carbon concentration in the retained austenite is responsible for its chemical stability, whereas its size and morphology determines its mechanical stability. Thus, to achieve the required mechanical properties, control of the processing parameters affecting the microstructure development is essential.

Introduction

Ever since the Transformation-Induced Plasticity (TRIP) effect was first reported by Zackay *et al*. [1] more than 50 years ago, significant research efforts have been directed towards understanding the mechanism and on the design of steel compositions and processing routes for its best utilisation. As a result, TRIP steels with lean compositions containing 0.15-0.2C-1.5-2Mn-1-1.5Si (wt.%) as the main elements and possible alloying additions of Al, Nb, Mo and P have been developed [2-5]. The microstructure of these steels consists of polygonal ferrite (PF), carbide-free bainite, retained austenite (RA) and possibly small amounts of martensite and cementite [6, 7]. These steels exhibit a good combination of strength and ductility (yield strength >550MPa, tensile strength >1000 MPa and total elongation between 25-40%) and high energy absorption [4,5]. In addition to the complex interactions between the multiple phases present in such TRIP steels, it is believed that the gradual transformation of metastable retained austenite during straining contributes significantly to the above mechanical properties [8-10]. As various processing schedules result in different microstructures, the focus of many research projects has been on increasing the volume fraction of the RA and its stability during straining [7,9,10]. Chemical (carbon content) and mechanical (size and morphology) stability of the RA are both important parameters that need to be controlled in order to achieve the desired strength-ductility balance in TRIP steels [7, 10-14]. In the present study, the correlation of the mechanical properties with the behaviour of the RA during tensile testing in thermo-mechanically processed TRIP steels is carried out.

Experimental Procedures

Three experimental TRIP steels with alloying additions of Al, Mo and Nb were used in this study (Table 1). They were subjected to laboratory rolling at 1100 °C (25% thickness reduction) and 950 °C (47% thickness reduction) after reheating to 1250 °C for 120 s. Then steels were cooled at $1Ks^{-1}$ (polygonal ferrite formation) to the temperature of accelerated cooling (T_{AC}), where the cooling rate was changed to ~50 Ks^{-1}. After reaching the isothermal holding temperature (T_{IH}) for bainite

formation, the steels were held at various times (t_{IH}) and then quenched. For NbMoAl steel, two T_{AC} were used in order to form 50 and ~15% of the PF. Hereafter, these conditions are referred to as NbMoAl-1and NbMoAl-2, respectively. Processing parameters are given in Table 1 and more details are available elsewhere [7, 15]. Tensile samples were machined from the thermo-mechanically processed strip. The microstructures of the steels after thermo-mechanical processing (TMP) [7] were investigated before and after straining using heat tinting [16] and X-ray diffraction (XRD) [17]. The steels in the TMP condition were also studied using thin foil transmission electron microscopy (TEM) [15] and atom probe tomography (APT) [15, 18]. NbMoAl-2 steel was also subjected to in-situ tensile testing on the 1ID high energy XRD beamline at the Advanced Photon Source, Argonne National Laboratory, USA [19].

Table 1: Steel compositions and processing parameters.

Steel		Element								Parameters		
		C	**Si**	**Mn**	**Mo**	**Al**	**Cu**	**Nb**	**P**	**T_{AC},°C**	**T_{IH},°C**	**t_{IH}, s**
Nb	**wt%**	0.21	1.48	1.5	**0.2**	0.01	0.02	**0.036**	0.025	735	450	1200
Mo	**at%**	0.96	2.88	1.49	**0.11**	0.02	0.017	**0.021**	0.044			
Nb	**wt%**	0.22	1.19	1.53	0.004	**0.57**	0.03	**0.037**	0.027	840	470	1800
Al	**at%**	1.00	2.31	1.52	0.002	**1.15**	0.026	**0.022**	0.048			
Nb Mo	**wt%**	0.21	1.18	1.52	**0.29**	**0.57**	0.03	**0.036**	0.027	760	470	1200
Al	**at%**	0.95	2.29	1.51	**0.17**	**1.15**	0.026	**0.021**	0.048	780		

T_{AC}- accelerated cooling start temperature; T_{IH}-isothermal hold temperature, t_{IH}-isothermal holding time

Results and Discussion

Characterisation of the microstructures after TMP The microstructures of all the steels after TMP contained ~50% of PF, carbide-free bainite, RA and martensite (Figs. 1a-1c, Table 2).

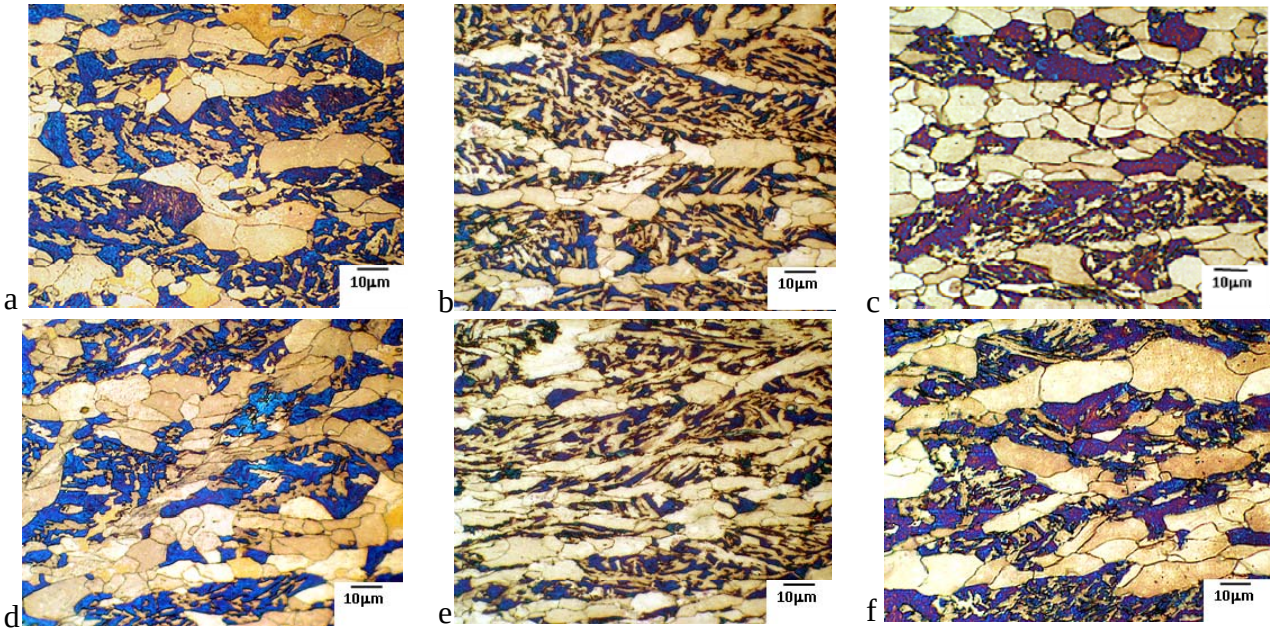

Fig. 1: Microstructures of NbMo (a,d), NbAl (b,e) and NbMoAl-1 (c,f) steels after thermo-mechanical processing (a-c) and after tensile test (d-f). Polygonal ferrite (PF) is light, bainitic ferrite (BF) is beige/brown, martensite (M) is blue and retained austenite (RA) is maroon.

However, compared to the Mo-containing steels, the NbAl steel has more refined PF as well as some Widmanstätten ferrite. While the bainite in all the steels was predominantly in the form of bainitic ferrite (BF) with M/RA layers between the laths (Figs. 2a and 2c), some granular bainite comprising BF plates with M/RA constituent phase was also present. The bainite microstructure was the coarsest in the NbMo steel and was the finest in the NbMoAl-1 steel. Some coarse blocks of RA were found in all the steels; especially at the PF/BF interfaces or in-between the PF grains (Fig. 2b). As the XRD study showed, the average carbon content was the highest and lowest in the NbMoAl-1 and NbAl steels, respectively, while the NbMoAl-2 steel contained ~8.5% of the RA with an intermediate level of carbon (Table 2). Incidentally, the latter steel also had the lowest amount of martensite. However, measurements of the different RA volumes in the steels using APT returned a wide variation in carbon content (2-3.6 at.%).

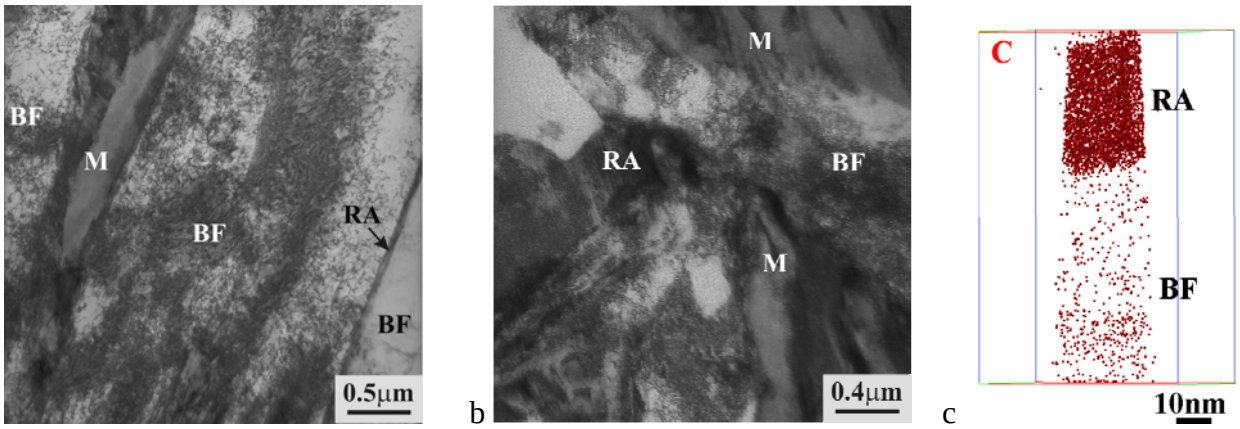

Fig. 2: Representative TEM micrographs (a,b) and C atom map (c) showing morphology of retained austenite: interlath (a,c) and blocky (b). BF-bainitic ferrite, RA- retained austenite and M-martensite.

Table 2: Summary of the mechanical properties and retained austenite/martensite characteristics.

Steel	**YS, MPa**	**UTS, MPa**	**Total / Uniform El., %**	**V_{RA}, %***	**V_M, %***	**RA Carbon Content, wt.%**	**V_{RA}, %†**
NbMo	420±20	1014±20	30/16±2	~12	~15	1.14	2
NbAl	460±30	1040±40	29/20±3	~7	~13	0.7	0
NbMoAl-1	555±30	1152±50	35/20±5	~12	~10	1.6	4.5
NbMoAl-2	718	1110	20.5/15.5	~8.5	~0.4	1.12	~1.3

**after TMP, †after tensile test*

Mechanical behaviour of the steels. All of the above steels recorded a very good combination of mechanical properties. The best balance of strength and elongation was found in the NbMoAl-1 steel, whereas the NbMo steel has the lowest uniform elongation. The NbMoAl-2 steel presented with high strength and lower ductility due to the lower amounts of PF and RA in its microstructure (Table 2, Fig. 3a). The values of the strain hardening coefficient (n) for all the steels are plotted against their true strains in Fig. 3b. It shows that the n values for the NbMo, NbAl and NbMoAl-1 steels increase rapidly up to a maximum right at the start of straining followed by a continuous decrease thereafter. Similar changes in n value were observed for intercritically annealed low-Si [8] and Fe-0.28C-1.41Si-1.5Mn (wt.%) [20] TRIP-assisted steels. On the other hand, the NbMoAl-2 steel exhibited an increase in n value from 0.15 to 0.2; which was maintained up to 0.06 strain followed by a very gradual decline.

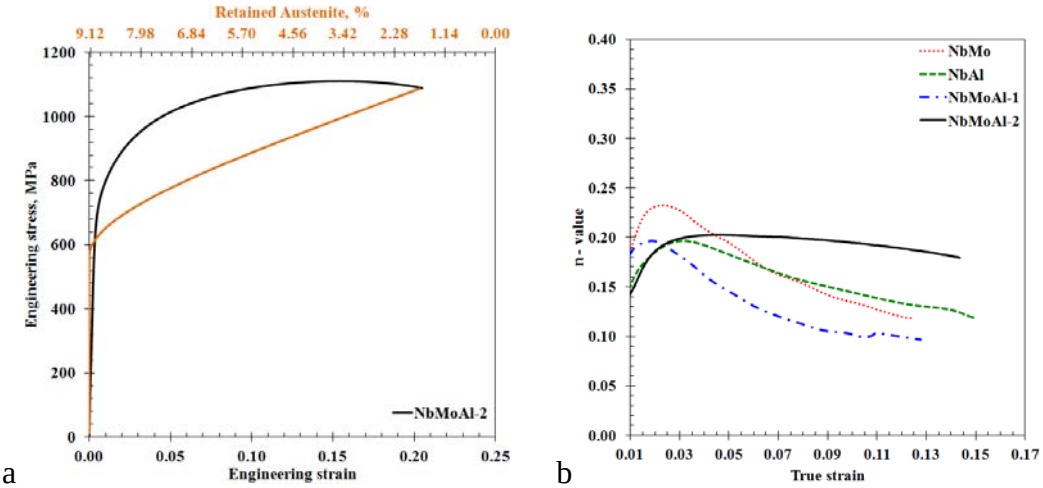

Fig. 3 Variation of stress and the retained austenite amount with engineering strain for the NbMoAl-2 steel (a) and n exponent behaviour for all studied steels (b).

Retained austenite stability. The evolution of the RA in the NbMoAl-2 steel was determined from XRD data collected during in-situ tensile testing (Fig. 3a), whereas the microstructures of the other three steels were examined at 0.05 and 0.12 true strain, as well as near the fracture surface. The NbMoAl-2 steel showed no change in the RA amount until ~600MPa; which is below its 0.2% proof stress of 718 MPa. This could be explained by the inhomogeneity of plastic deformation and that the local stresses required for both, plastic deformation and the initiation of deformation-induced transformation of austenite to martensite were reached earlier on a local level than when macroscopic yielding was detected. It also may indicate stress-induced rather than strain-induced transformation. From ~600 MPa to >1100 MPa the amount of the RA decreased gradually such that ~1.3% remained in the microstructure after fracture. This gradual transformation of the RA is responsible for the observed high values of n exponent.

In NbMo steel, most of the retained austenite transformed to martensite at 0.05 strain; which accounts for the sharp increase in the n value to its maximum of ~0.24. However, ~ 2% of RA remained in the microstructure after tensile testing (Table 2, Fig. 1d). Early and fast transformation of the RA could be explained by the relatively low chemical (1.14 wt.% C) and mechanical stability as the external stress propagated directly to the RA through the hard martensite phase; which then increased the total driving force for the retained austenite to transform to martensite [21]. Since the bainitic structure was very rigid and did not elongate during deformation, an increase in load transfer to the interlath RA can also be expected. On the other hand, the PF and bainite in the NbAl steel were relatively soft and easily plastically deformed during the tensile test (Fig. 1e). Although, the rate of the RA transformation to martensite was slower than in NbMo steel, all of it transformed to martensite at low strains due to its very low chemical stability (0.7 wt.% C). The transformation of the RA to martensite in the NbMoAl-1 steel occurred gradually: ~8% of retained austenite was present at the intermediate level of the deformation whereas ~5% of retained austenite was observed at ~0.27 strain and ~4.5% of the RA remained in the microstructure at fracture. In comparison to NbMoAl-2, the higher volume fraction of PF led to a larger amount of carbon being rejected into the RA; thereby causing its chemical stabilisation and allowing it to remain untransformed. As could be seen from Fig. 1f, the majority of coarse blocky RA located between the PF grains or at the PF/BF interface have transformed to martensite whereas some of the RA located within the bainitic structure remain untransformed. The coarse blocky RA crystals tend to be less enriched in carbon compared to the RA located within the bainite; as the latter benefit from carbon enrichment from both ferrite and bainite phase transformations. In addition, the fine islands of austenite that are trapped between the plates of bainitic ferrite in a sheaf are much more stable not only due to the higher carbon concentration but also because of the physical constraint to transformation due to the close proximity of plates in all directions [22]. Comparable behaviour in the RA stability with respect to its location and morphology was observed for similarly processed

non-Nb TRIP and Nb-containing steels [7]. However, very fine RA islands or RA with very high carbon content are over-stabilised and do not contribute to the TRIP effect. Thus, it is important to form RA with emphasis on particular morphology, size and carbon content in order to provide a more gradual transformation to martensite during strain such that it enables the maximising of the TRIP effect.

Conclusions

The results have shown that the chemical inhomogeneity of the RA depends on its location in the complex microstructure of multi-phase steels which together with morphology and size controls the rate of the RA transformation to martensite upon straining. In addition, the RA stability also depends on the properties of the surrounding phases and their interactions with respect to the overall load transfer.

Acknowledgement

Support by the Australian Synchrotron Research Program, the XOR beamline members, Dr K.-D. Liss from ANSTO, the APS user office and Monash Centre for Electron Microscopy is gratefully acknowledged.

References

[1] V.F. Zackay, E.R. Parker, D. Fahr and R. Bush, Trans. Am. Soc. Met., 60 (1967) 252-259.
[2] W.W. Gerberich, P.L. Hemmings, M.D. Merz, V.F. Zackay, Trans. Techn. Notes, 61 (1968) 843-47.
[3] H.K.D.H. Bhadeshia, D.V. Edmonds, Metall. Trans., 10A (1979) 895-907.
[4] Y. Sakuma, O. Matsumura, H. Takechi, Metall. Trans. A, 22A (1991) 489-98.
[5] B.C. De Cooman, Curr. Opin. Solid State Mater. Sci., 8 (2004) 285-303.
[6] S.K. Liu and J. Zhang, Metall. Trans. A, 21A (1990) 1517-25.
[7] I.B. Timokhina, P.D. Hodgson, E.V. Pereloma, Metall. Mater. Trans. A, 35A (2004) 2331-2341.
[8] P.J. Jacques, J. Ladrière, F. Delanny, Metall. Mater. Trans. A, 32A (2001) 2759-2768.
[9] O. Matsumura, Y. Sakuma, Y. Ishii, J. Zhao, Iron Steel Inst. Jpn. Int., 32 (1992) 1110-16.
[10] E. Pereloma, H. Belladi, L. Zhang, I. Timokhina, Metall. Mater. Trans. A, 43A (2012) 3958-3971.
[11] G. Reisner, E. A. Werner, P. Kerschbaummaur, I. Papst, F.D. Fischer, I. Met., 49 (1997) 62-65.
[12] M. De Meyer, D. Vanderschueren, B.C. De Cooman, Iron Steel Inst. Jpn. Int., 39 (1999) 813-22.
[13] H.C. Chen, H. Era, and M. Shimizu, Metall. Trans. A, 20A (1989) 437-45.
[14] V.T.T. Miihkinen and D.V. Edmonds, Mater. Sci. Technol., 3 (1987) 422-30.
[15] E.V. Pereloma, I.B. Timokhina, M.K. Miller, P.D. Hodgson, Acta Mater., 55 (2007) 2587-2598.
[16] B.V. Kovacs, On the terminology and structure of ADI, Trans. AFS, 102 (1994) 417- 420.
[17] B.D. Cullity, Elements of X-Ray Diffraction, Addison-Wesley Publishing Company Inc., 1978, p. 555.
[18] M.K. Miller, Atom Probe Tomography, Kluwer, Academic/Plenum Press, New York, 2000.
[19] E. Pereloma, L. Zhang, K.-D. Liss, U. Garbe, J. Almer, T. Chambron, H. Beladi, and I. Timokhina, Solid State Phenomena, 172-174 (2011) 741-46.
[20] J. H. Chung, J.B. Jeon, Y. W. Chang, Met. Mater. Int., Vol. 16, No. 4 (2010), pp. 533~541
[21] I. Tsukatani, S. Hashimoto, T. Inoue, ISIJ International, 31 (1991) 992-1000.
[22] M. Takahashi and H.K.D.H. Bhadeshia, Materials Transactions, JIM, 32 (1991) 689-696.